

A NON-INVERTING BUCK-BOOST CONVERTER WITH AN ADAPTIVE DUAL CURRENT MODE CONTROL

Srdan Lale¹, Milomir Šoja¹, Slobodan Lubura¹,
Dragan D. Mančić², Milan Đ. Radmanović²

¹University of East Sarajevo, Faculty of Electrical Engineering, East Sarajevo,
Bosnia and Herzegovina

²University of Niš, Faculty of Electronic Engineering, Niš, Serbia

Abstract. *This paper presents an implementation of adaptive dual current mode control (ADCMC) on non-inverting buck-boost converter. A verification of the converter operation with the proposed ADCMC has been performed in steady state and during the disturbances in the input voltage and the load resistance. The given simulation and experimental results confirm the effectiveness of the proposed control method.*

Key words: *adaptive dual current mode control, non-inverting buck-boost converter, operating modes, transient response*

1. INTRODUCTION

A non-inverting buck-boost power electronics converter is one of the most versatile non-isolated converter topologies. It has become increasingly popular in many applications, including: electric vehicles [1], DC microgrids [2], battery-powered portable electronic devices (e.g. cellular phones and laptops) [3], [4], power factor correction (PFC) circuits [5], photovoltaic systems [6], etc. The non-inverting buck-boost converter provides the output voltage that is either lower or higher than the input voltage. This property is significant in so-called dynamic voltage scaling (DVS)-based power-efficient supplies, which provide adjustable voltage levels, according to the instantaneous operating conditions [7]. One of the most important features of this converter type is bidirectional operation, which is especially useful in applications such as DC microgrids and electric vehicles.

The conventional two-switch topology of the non-inverting buck-boost converter is shown in Fig. 1 (a), being a result of a cascaded combination of a buck converter followed by a boost converter. It contains two power switches T_1 and T_2 . If a bidirectional operation of the non-inverting buck-boost converter is required, a four-switch topology from Fig. 1 (b) must be used,

Received January 25, 2016; received in revised form April 10, 2016

Corresponding author: Srdan Lale

University of East Sarajevo, Faculty of Electrical Engineering, Vuka Karadžića 30, 71126 Lukavica, East Sarajevo
Bosnia and Herzegovina

(E-mail: srdjan.lale@etf.unssa.rs.ba)

where the diodes D_1 and D_2 from Fig. 1 (a) are replaced with additional power switches T_3 and T_4 .

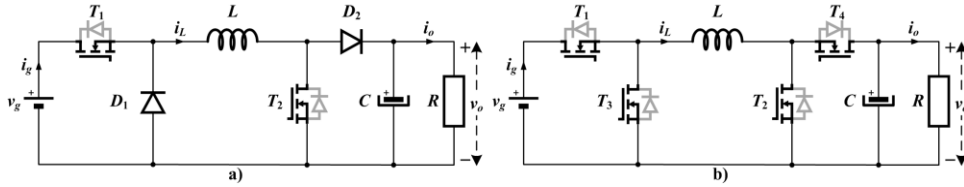


Fig. 1 A 2-switch (a) and 4-switch (b) topology of the non-inverting buck-boost converter

Depending on the ratio between the input voltage v_g and the output voltage v_o , the non-inverting buck-boost converter can operate in buck mode ($v_o < v_g$) or boost mode ($v_o > v_g$). As it is discussed in [8], these operating modes can be achieved in different ways. A conventional way is to control simultaneously the switches T_1 and T_2 with the same gate signal. Although this switching scheme is simple, it provides low converter efficiency. In order to increase the efficiency, the operating modes are split: converter operates either as buck converter (only switch T_1 is controlled, while T_2 is always turned off) when $v_o < v_g$ or boost converter (only switch T_2 is controlled, while T_1 is always turned on) when $v_o > v_g$. However, the control of the switches is more complicated in this case, because it is necessary to provide mode detection and smooth and stable transition between the modes.

Different control methods can be applied to the non-inverting buck-boost converter, depending on the application. This paper is focused on using only current mode control (CMC). In most cases, for example in [2], [3], [5], [9], regardless of the applied CMC method, it is suggested that the non-inverting buck-boost converter operates either as buck or boost converter, as described above. In [5], a non-inverting buck-boost converter as a part of PFC rectifier works in both modes during fundamental period. After detection of each operating mode, the built-in control logic decides to work as conventional peak CMC (PCMC) or valley CMC (VCMC). Therefore, the control shifts between PCMC (boost mode with duty cycle below 0.5) and VCMC (buck mode with duty cycle above 0.5) when the input rectified voltage crosses the output DC voltage, without need for slope compensation. In [9] a synchronous buck-boost LED driver controller is presented, which uses more complex control as a combination of PCMC and VCMC with slope compensation.

However, as it is stated in [2], an implementation of conventional CMC methods to this converter, such as PCMC and VCMC, is not a simple task, because they require information about converter operating modes. An average CMC (ACMC) can be applied to the non-inverting buck-boost converter, without determination of operating modes [2]. By using a dual-carrier modulator described in [2], it is possible to achieve a smooth transition between the buck and the boost mode and to precisely control the inductor current throughout the entire operating range. There are other ACMC approaches, for example in [3], which unlike the above mentioned ACMC [2] has a mode selector circuit, which determines the operating mode during a switching cycle.

Due to the inherent ability of natural transition between PCMC and VCMC and vice versa, a dual current mode control (DCMC) proposed in [10] could be suitable for implementation on the non-inverting buck-boost converter, with simultaneously controlled

switches T_1 and T_2 . The converter will operate in buck mode with PCMC (duty cycle below 0.5) and in boost mode with VCMC (duty cycle above 0.5). In this way, there is no need for detection of operating modes. Also, the converter is stable for the entire range of duty cycle from 0 to 1, that is, the subharmonic oscillations do not exist. On the other hand, all excellent features of PCMC and VCMC are preserved, such as fixed switching frequency, good dynamics and what is very important - simplicity.

A modified version of DCMC, named adaptive dual current mode control (ADCMC), is proposed in [11] and elaborated in detail in [12], which improves some features of DCMC, while the basic operating principles remain the same. In [12], only simulation results are given for the non-inverting buck-boost converter. In this paper, besides some simulation results, the experimental verification of ADCMC of this converter is presented.

The paper is organized in the following way. The basic operating principles of ADCMC, on the example of the non-inverting buck-boost converter, are described in Section 2. The simulation and experimental results are presented in Section 3. Section 4 gives the concluding remarks.

2. OPERATING PRINCIPLES OF ADCMC OF NON-INVERTING BUCK-BOOST CONVERTER

The basic scheme of ADCMC of the conventional non-inverting buck-boost converter is presented in Fig. 2 (a). The switches T_1 and T_2 are controlled simultaneously with the same gate signal. In order to increase the converter efficiency, there is a possibility of synchronous version of this converter, where the diodes D_1 and D_2 are replaced with power switches, as it is shown in Fig. 1 (b). In this paper, a synchronous version is not used. However, as it is stated in the Introduction, if bidirectional operation of the non-inverting buck-boost converter is required, these additional two switches are necessary.

A quiescent value of the output voltage V_o of the non-inverting buck-boost converter from Fig. 2 (a) is equal to:

$$V_o = \frac{DV_g}{1-D}, \quad (1)$$

where D and V_g are the quiescent values of the duty cycle and the input voltage, respectively. According to (1), when $0 < D < 0.5$, the output voltage is lower than the input voltage and the converter works in buck mode. When $0.5 < D < 1$, the output voltage is higher than the input voltage and the converter works in boost mode. If $D=0.5$, the input and output voltages are equal.

By choosing PCMC for $D < 0.5$ (buck mode) and VCMC for $D > 0.5$ (boost mode), a stable operation of the non-inverting buck-boost converter is guaranteed for the entire range of D without slope compensation. Instead of mode detection and artificial shifting between PCMC and VCMC, DCMC proposed in [10] is suitable for this application, because it has a natural ability of shifting between PCMC, when $D < 0.5$, and VCMC, when $D > 0.5$, without any mode selector circuits.

Similarly as PCMC and VCMC, DCMC has a drawback in existence of a peak-to-average current error (a difference between the reference current i_{ref} and the average value of the inductor current $\langle i_L(t) \rangle_{T_s}$ over switching period T_s). In ideal case of CMC, the aim is

to control precisely the average value of the inductor current over each switching period, that is, to make this error equal to zero. In order to eliminate peak-to-average current error, an enhanced version of DCMC is proposed in [11], named ADCMC.

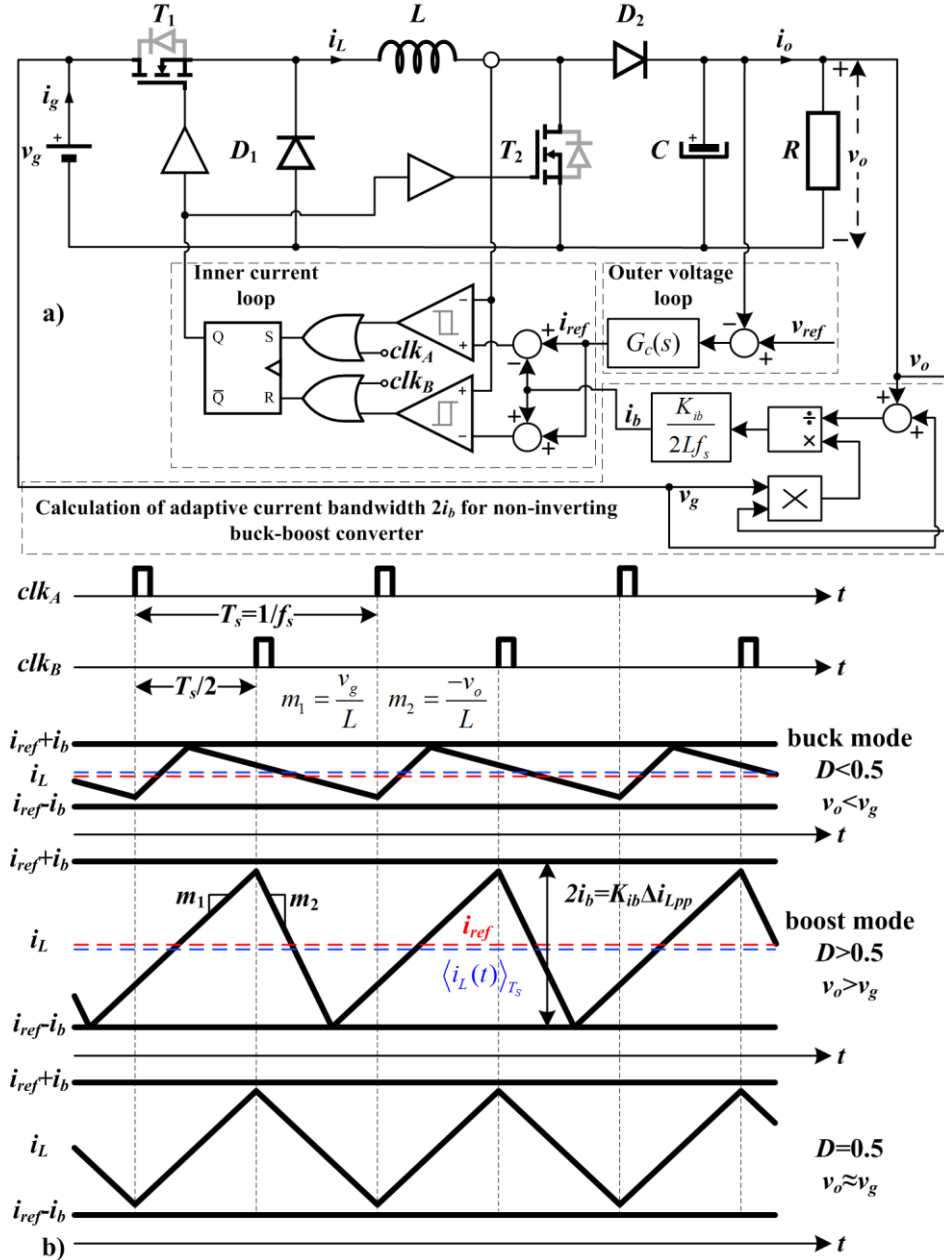


Fig. 2 a) ADCMC of the non-inverting buck-boost converter, b) Operating modes

The operating modes of ADCMC applied to the non-inverting buck-boost converter are shown in Fig. 2 (b). The main difference between ADCMC and DCMC is in the fact that the width between peak $i_{ref}+i_b$ and valley $i_{ref}-i_b$ current boundaries (the current bandwidth $2i_b$), is not constant and predefined for ADCMC, unlike DCMC, but it is adaptive and online calculated by using the instantaneous peak-to-peak ripple of the inductor current Δi_{Lpp} on each switching period T_s . The adaptive current bandwidth $2i_b$ for the non-inverting buck-boost converter is calculated as (Fig. 2 (a)):

$$2i_b = K_{ib} \Delta i_{Lpp} = K_{ib} \frac{v_g v_o}{L f_s (v_g + v_o)}, \quad (2)$$

where K_{ib} is the scaling gain ($K_{ib} \geq 1$), $f_s = 1/T_s$ is the switching frequency, and L is the inductance value. The gain K_{ib} determines whether $2i_b \geq \Delta i_{Lpp}$. When $K_{ib} = 1$, the adaptive current bandwidth $2i_b$ becomes equal to the measured instantaneous peak-to-peak current ripple Δi_{Lpp} , giving zero peak-to-average current error.

It is evident from (2) that the calculation of adaptive current bandwidth $2i_b$ depends on the inductance value L , which can be inconvenient if the L parameter is wrong or variable in different operating conditions. The wrong L parameter will lead to inaccurate current bandwidth $2i_b$ and the appearance of the peak-to-average current error. A possible solution for this issue is to directly measure the instantaneous peak-to-peak ripple from the measured inductor current. This solution will be considered in the future work.

A detailed analysis of ADCMC, including small-signal models and design of the output voltage compensator $G_c(s)$ are presented in [12] for three types of DC-DC power electronics converters: buck, boost, and non-inverting buck-boost converter. This paper is focused on experimental verification of ADCMC of non-inverting buck-boost converter.

3. SIMULATION AND EXPERIMENTAL RESULTS

The operation of the non-inverting buck-boost converter under ADCMC, with the topology from Fig. 2 (a), was verified with simulations in Matlab/Simulink and experimentally. The parameters of the non-inverting buck-boost converter working in the continuous conduction mode (CCM), which are the same for both simulations and experiments, are listed in Table 1.

The experimental setup is shown in Fig. 3. The developed setup can be used for testing ADCMC on various types of converters, because the used prototype is made as a universal four-quadrant (4Q) converter, with possibility of easy configuration to the desired topology, such as buck, boost, non-inverting buck-boost, etc.

Table 1 Parameters of the non-inverting buck-boost converter

V_g [V]	12
L [μ H]	220
C [μ F]	1000
R [Ω]	20
f_s [kHz]	23

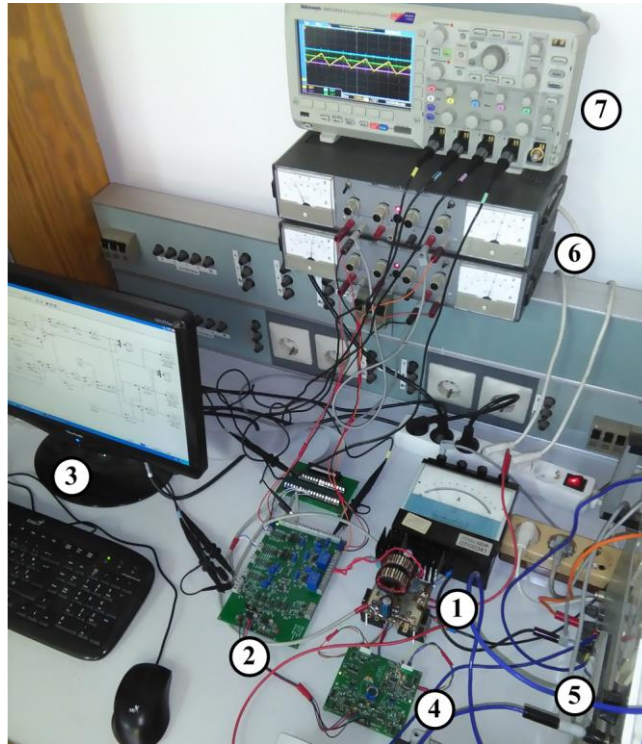


Fig. 3 Experimental setup: 1) The prototype of the non-inverting buck-boost converter; 2) Electronic module for measurements and inner current loop; 3) PC with built-in MF624 board; 4) Driver module; 5) Input voltage source of the converter; 6) Power supply units; 7) Tektronix MSO 2014 oscilloscope

A separate electronic module, which is connected to MF624 multifunctional data acquisition input/output digital board [13], is used for implementation of the measurements and inner current loop. The measurement of the inductor current, which is necessary for the inner current loop, is performed with LEM current transducer HX 10-NP [14]. The converter input and output voltage are measured with galvanic isolation via optocoupler IL300 [15] and sampled by 14-bit A/D converter (conversion time about 2 μ s) of the MF624 board. MF624 board is built into the computer and it provides a real time processing with Matlab/Simulink environment. An implementation of the outer voltage loop and calculation of the adaptive current bandwidth $2i_b$ for ADCMC is performed in real time in Simulink, using Real Time Windows Target (RTWT) environment. The reference current i_{ref} and current boundaries $i_{ref}+i_b$ and $i_{ref}-i_b$ are obtained from 14-bit D/A converter of the MF624 board and fed into the inner current loop. The fundamental sampling time for real time operation in Simulink was set to 25 μ s, which is the minimum sampling time for this hardware.

Power MOSFETs IRF540N (100 V, 33 A) [16] are used as power switches T_1 and T_2 . A dual-channel galvanically isolated MOSFET driver module (turn on/off delay of 0.6 μ s) was developed for driving the power switches.

A primary objective of the performed simulations and experiments is to demonstrate that the proposed ADCMC can be successfully applied to the non-inverting buck-boost converter, ensuring a stable operation in all operating modes and good dynamical properties, regardless of the application. Several cases of the converter operation were tested: in steady state for buck and boost operating modes, during the step changes in the input voltage and the load resistance and during the gradual change of the input voltage.

3.1. Operation of the non-inverting buck-boost converter in steady state

The output compensator, as a key part of the outer voltage loop, produces the reference current i_{ref} for the inner current loop (Fig. 2 (a)). In steady state, the reference current practically has a constant value. Therefore, in order to test the behavior of the inner current loop in steady state, the outer voltage loop can be disabled and the reference current should be set manually as a constant signal.

A testing the operation of the non-inverting buck-boost converter with ADCMC in steady state was performed for both cases: with and without the outer voltage loop. When the voltage loop is disabled, two values of the reference current were used to provide buck and boost operating mode. The simulation waveforms of the inductor current in steady state are shown for $i_{ref}=0.5$ A (buck mode) in Fig. 4 (a) and $i_{ref}=5$ A (boost mode) in Fig. 4 (b). The corresponding experimental waveforms are given in Fig. 5 (a), (b).

In the second case, a simple proportional-integral (PI) compensator for the regulation of the output voltage was employed. A design procedure for the output voltage compensator is derived in detail in [12]. As in the first case, the both operating modes were considered. The simulation waveforms of the inductor current in steady state are shown for two values of the output voltage: $v_o=7$ V (buck mode) and $v_o=30$ V (boost mode), in Fig. 4 (c) and Fig. 4 (d), respectively. The corresponding experimental results are presented in Fig. 5 (c), (d).

It is evident from Fig. 4 that there is an excellent matching between the reference current and the average value of the inductor current. A very small peak-to-average current error still exists, which can be attributed to the delays in numerical calculation of the simulation.

The experimental results from Fig. 5 are similar to the simulation results from Fig. 4. A small peak-to-average current error appears as a consequence of imperfections of the components used for realization of ADCMC.

On the basis of the given results from Fig. 4 and Fig. 5 it can be concluded that ADCMC provide a stable operation of the non-inverting buck-boost converter for both values of the duty cycle: $D < 0.5$ and $D > 0.5$.

3.2. Robustness to the disturbances in the input voltage and load

It is very important to evaluate how the converter with certain control is sensitive to the various disturbances which can occur during operation. In this paper, the disturbances such as the step and gradual changes of the input voltage and the step changes in the load resistance were considered.

A line regulation, which is defined as converter ability to maintain the specified output voltage despite changes in the input voltage, was tested for ADCMC of the non-inverting buck-boost converter.

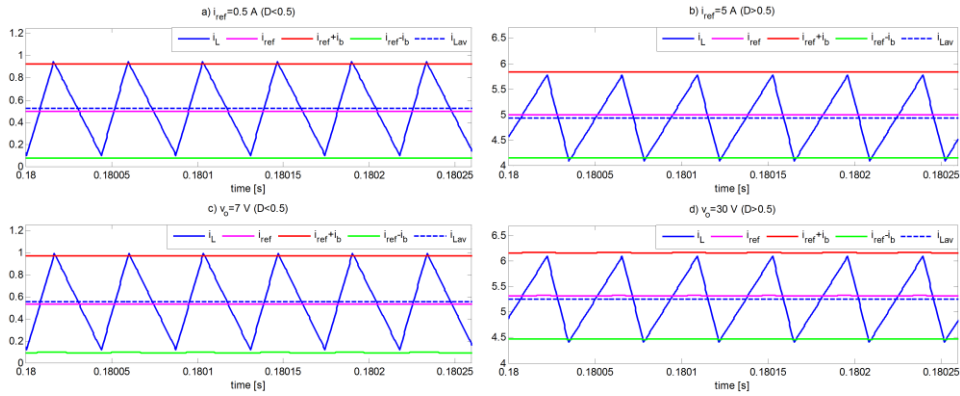


Fig. 4 The simulation waveforms of the inductor current, reference current and current boundaries in steady state, when the outer voltage loop is: a), b) disabled; c), d) enabled

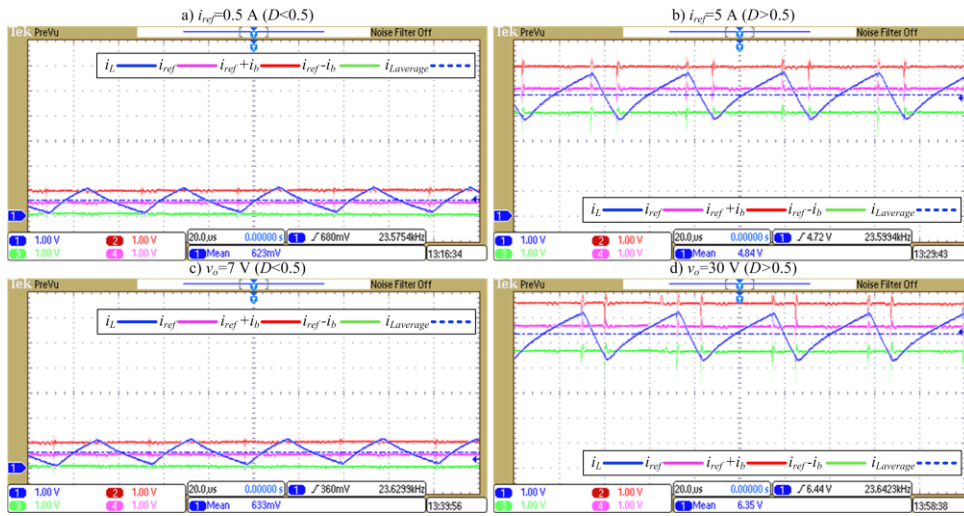


Fig. 5 The experimental waveforms of the inductor current, reference current and current boundaries in steady state, when the outer voltage loop is: a), b) disabled; c), d) enabled

First, the step changes from 12 V to 6 V and vice versa, were introduced in the input voltage. The output voltage was regulated to 9 V. The load resistance was set to $R=10\ \Omega$. These step changes were performed in order to make a transition from buck to boost mode and vice versa, and to examine the dynamical behavior of ADCMC. The waveforms of the output voltage and the inductor current are shown in Fig. 6 (a), (b) (simulation) and Fig. 7 (experiment). The same parameters of the output voltage compensator were used in both simulations and experiments.

As it is shown from simulation and experimental results, the converter naturally crosses from buck to boost mode and vice versa. Due to adaptation of the current bandwidth $2i_b$, the transition of the inductor current from one mode to another is smooth, which gives satisfactory line regulation.

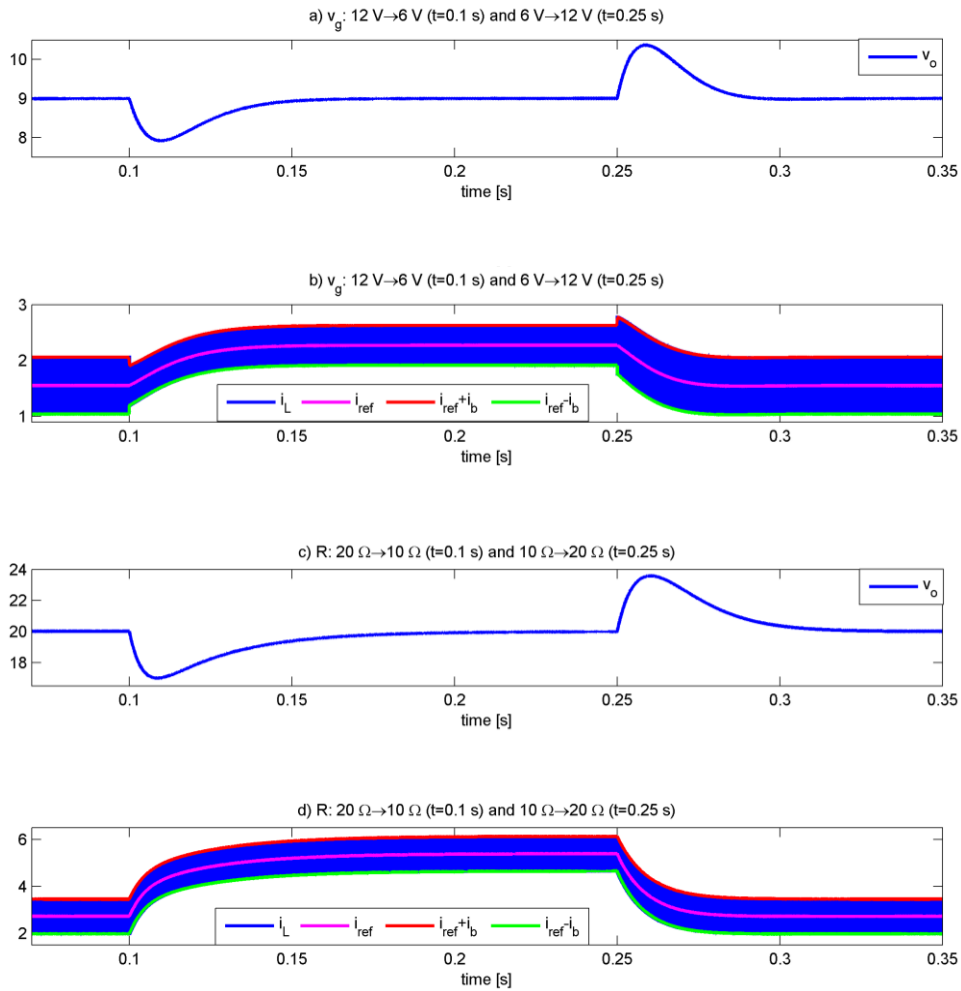


Fig. 6 The simulation waveforms of the output voltage and the inductor current, for the step changes in the input voltage (a), (b) and the load resistance (c), (d)

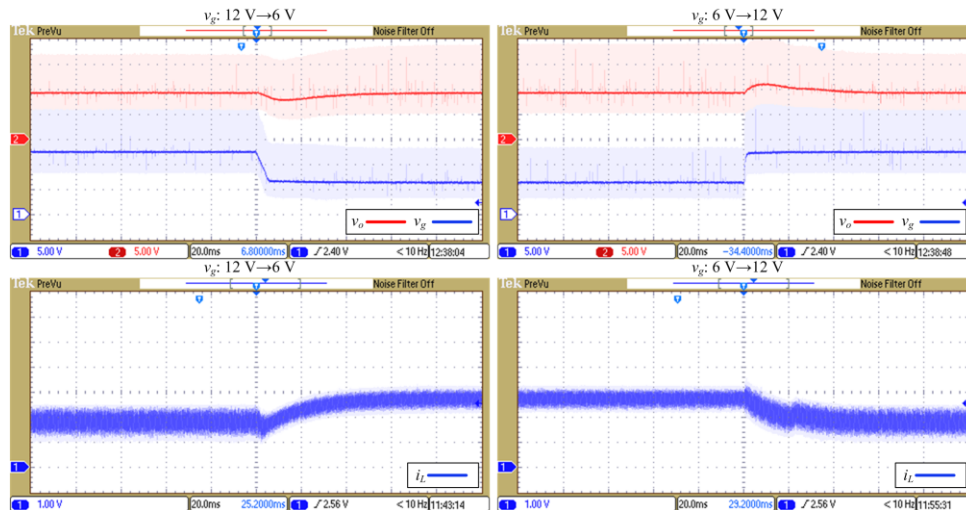


Fig. 7 The experimental waveforms of the output voltage (up) and the inductor current (bottom), when the input voltage changes from 12 V to 6 V (left) and vice versa (right)

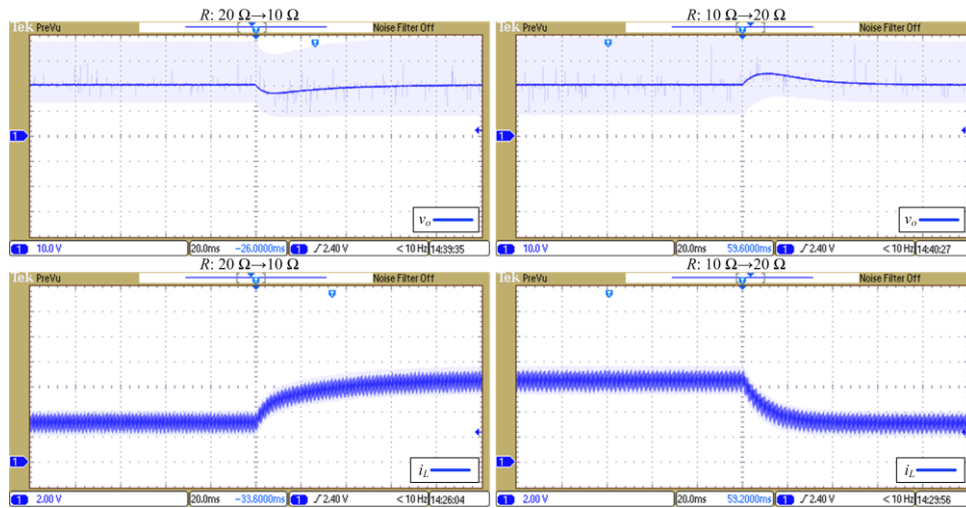


Fig. 8 The experimental waveforms of the output voltage (up) and the inductor current (bottom), when the load resistance changes from 20 Ω to 10 Ω (left) and vice versa (right)

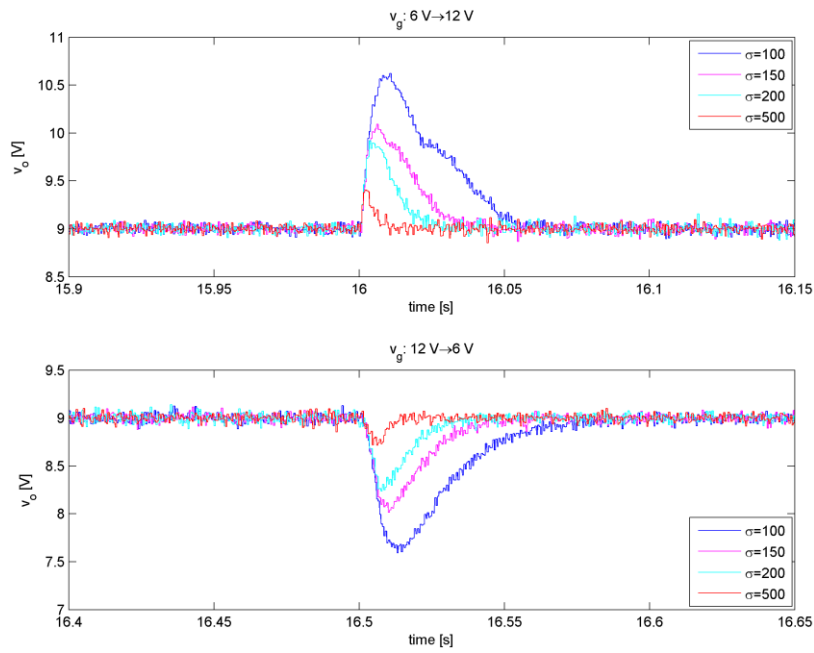


Fig. 9 The experimental waveforms of the output voltage, when the input voltage changes from 6 V to 12 V (up) and vice versa (bottom), for $\sigma=100, 150, 200$ and 500

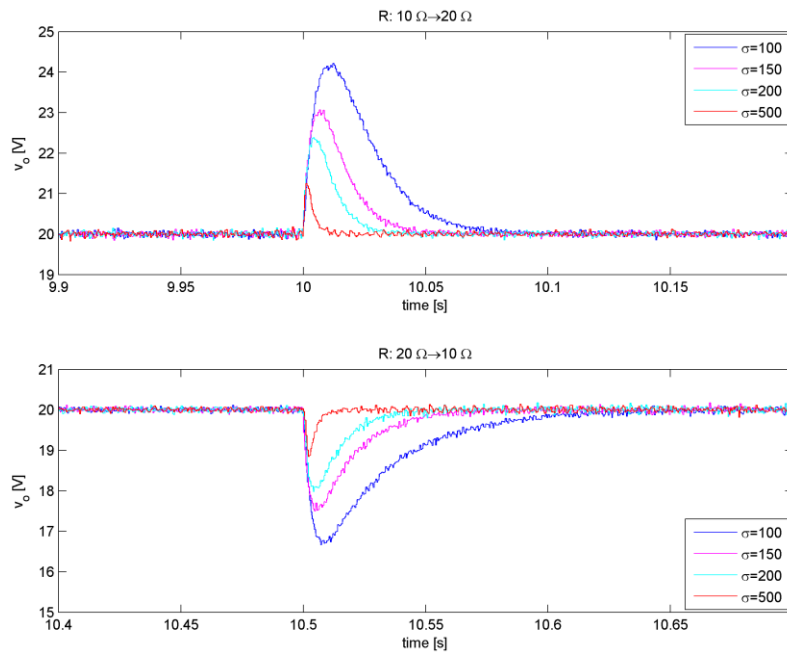


Fig. 10 The experimental waveforms of the output voltage, when the load resistance changes from 10 Ω to 20 Ω (up) and vice versa (bottom), for $\sigma=100, 150, 200$ and 500

In order to test a step load response, step changes in the load resistance from $R=20\ \Omega$ to $R=10\ \Omega$ and vice versa were performed. The output voltage was regulated to 20 V. The simulation and experimental waveforms of the output voltage and the inductor current are shown in Fig. 6 (c), (d) and Fig. 8, respectively. It is evident that ADCMC successfully reject the introduced load disturbances.

The transient response in the output voltage for the considered step disturbances depends also on the designed output voltage compensator, as it is shown in Fig. 9 and Fig. 10. Several values of parameter σ , which determines the transient response time (about $5/\sigma$) and the gains of the PI compensator [12], are considered.

It is evident from the given experimental results from Fig. 9 and Fig. 10 that better responses regarding the transient response time and over/undershoot are obtained for higher values of the adjustable parameter σ .

The optimization of the output voltage compensator is not subject in this paper. The aim was to obtain satisfactory results in accordance with the design procedure from [12] (the chosen settling time is about 10-50 ms). Also, the output voltage loop is designed to be slow in order to emphasize the behavior of the inner current loop.

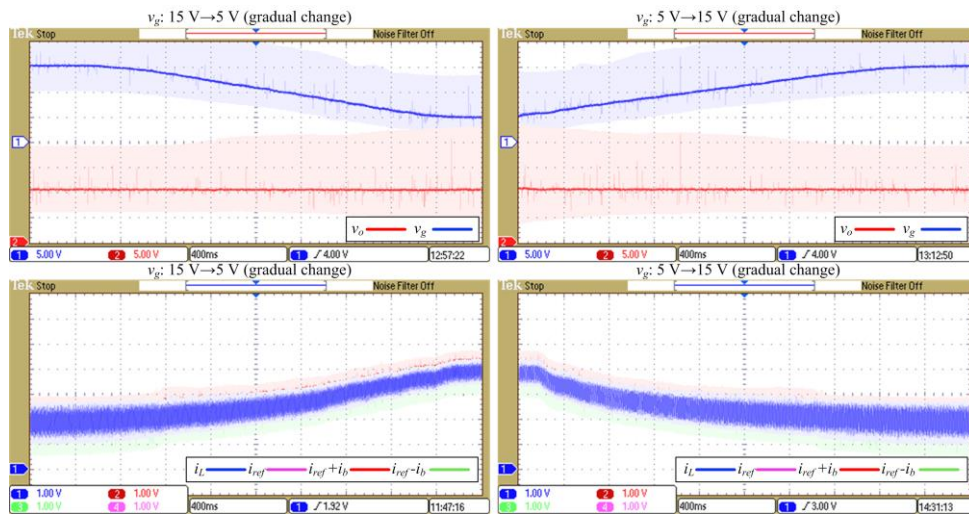


Fig. 11 The experimental waveforms of the output voltage (up) and the inductor current (bottom), for the gradual change of the input voltage from 15 V to 5 V (left) and vice versa (right)

Besides the step changes, a gradual linear change in the input voltage was also introduced in the experiments. The input voltage was gradually changed from 15 V to 5 V and vice versa, while the output voltage was regulated to 10 V, in order to make a gradual transition from buck to boost mode and vice versa. The experimental results are shown in Fig. 11. It is obvious that ADCMC is robust against these changes. The output voltage is successfully regulated, without any disruptions between two operating modes.

4. CONCLUSION

In this paper, an implementation of a novel ADCMC method on the non-inverting buck-boost converter has been presented. The given simulation and experimental results confirm that there is no need for the detection of converter operating modes, because this method ensures a natural and stable transition between the buck and the boost mode, and vice versa. The given results show that ADCMC provides a stable operation of the non-inverting buck-boost converter for the entire range of duty cycle from 0 to 1. Also, it is robust against the disturbances, such as the step and gradual changes in the input voltage and the step changes in the load resistance, with good dynamical performances.

The following task will be the using of the proposed ADCMC of the non-inverting buck-boost converter in various popular applications, such as battery chargers/dischargers, LED drivers, etc., and to compare it with other relevant methods in the same applications.

REFERENCES

- [1] M. A. Khan, A. Ahmed, I. Husain, Y. Sozer and M. Badawy, "Performance Analysis of Bidirectional DC–DC Converters for Electric Vehicles", *IEEE Trans. Ind. Appl.*, vol. 51, no. 4, pp. 3442-3452, July/Aug. 2015.
- [2] I. Aharon, A. Kuperman and D. Shmilovitz, "Analysis of Dual-Carrier Modulator for Bidirectional Noninverting Buck–Boost Converter", *IEEE Trans. Power Electron.*, vol. 30, no. 2, pp. 840-848, Feb. 2015.
- [3] Wei Chia-Ling, Chen Chin-Hong, Wu Kuo-Chun and Ko I-Ting, "Design of an Average-Current-Mode Noninverting Buck–Boost DC–DC Converter With Reduced Switching and Conduction Losses", *IEEE Trans. Power Electron.*, vol. 27, no. 12, pp. 4934-4943.
- [4] C.-H. Tsai, Y.-S. Tsai and H.-C. Liu, "A Stable Mode-Transition Technique for a Digitally Controlled Non-Inverting Buck–Boost DC–DC Converter", *IEEE Trans. Ind. Electron.*, vol. 62, no. 1, pp. 475-483, Jan. 2015.
- [5] G. K. Andersen and F. Blaabjerg, "Current programmed control of a single-phase two-switch buck-boost power factor correction circuit", *IEEE Trans. Ind. Electron.*, vol. 53, no. 1, pp. 263-271, Feb. 2006.
- [6] T.-F. Wu, C.-L. Kuo, K.-H. Sun, Y.-K. Chen, Y.-R. Chang and Y.-D. Lee, "Integration and Operation of a Single-Phase Bidirectional Inverter With Two Buck/Boost MPPTs for DC-Distribution Applications", *IEEE Trans. Power Electron.*, vol. 28, no. 11, pp. 5098-5106, Nov. 2013.
- [7] L. Feng and M. Dongsheng, "Design of Digital Tri-mode Adaptive-Output Buck–Boost Power Converter for Power-Efficient Integrated Systems", *IEEE Trans. Ind. Electron.*, vol. 57, no. 6, pp. 2151-2160, June 2010.
- [8] Haifeng Fan, "Design tips for an efficient non-inverting buck-boost converter", *Analog Applications Journal*, Texas Instruments, pp. 20-25, 2014.
- [9] Linear Technology, "60V 4-Switch Synchronous Buck-Boost LED Driver Controller", LT3791 datasheet, Rev. B, 2012. Available: <http://cds.linear.com/docs/en/datasheet/3791fb.pdf>.
- [10] A. V. Anunciada and M. M. Silva, "A new current mode control process and applications", *IEEE Trans. Power Electron.*, vol. 6, no. 4, pp. 601–610, Oct. 1991.
- [11] S. Lale, M. Šoja, S. Lubura and M. Radmanović, "Modeling and analysis of new adaptive dual current mode control", In Proceedings of the 10th International Symposium on Industrial Electronics INDEL 2014, vol. 10, no. T-02, pp. 73–76.
- [12] Available: http://www.indel.etfbl.net/resources/Proceedings_2014/INDEL_2014_Paper_11.pdf.
- [13] S. Lale, M. Šoja and S. Lubura, "A modified dual current mode control method with an adaptive current bandwidth", *Int. J. Circ. Theor. Appl.*, 2015.
- [14] HUMUSOFT, "MF624 Multifunction I/O Card", MF624 user's manual, 2014. Available: <http://www2.humusoft.cz/www/datacq/manuals/mf624um.pdf>.
- [15] LEM, "Current Transducer HX 05..15-NP", HX 10-NP datasheet. Available: http://www.lem.com/docs/products/hx%205_15-np_e%20v10.pdf.

- [16] Vishay Semiconductors, "Linear Optocoupler, High Gain Stability, Wide Bandwidth", IL300 datasheet. Available: <http://www.vishay.com/docs/83622/il300.pdf>.
- [17] International Rectifier, "HEXFET[®] Power MOSFET", IRF540N datasheet. Available: <http://www.irf.com/product-info/datasheets/data/irf540n.pdf>.